Journal of Arrhythmia 32 (2016) 443–448

Contents lists available at ScienceDirect

Journal of Arrhythmia

journal homepage: www.elsevier.com/locate/joa

Review

Catheter ablation of anteroseptal accessory pathways from the aortic cusps: A case series and a review of the literature

Konstantinos P. Letsas, MD*, Michael Efremidis, MD, Konstantinos Vlachos, MD, Stamatis Georgopoulos, MD, Nikolaos Karamichalakis, MD, Athanasios Saplaouras, MD, Sotirios Xydonas, MD, Kosmas Valkanas, MD, Antonios Sideris, MD

Second Department of Cardiology, Laboratory of Cardiac Electrophysiology, Evangelismos General Hospital of Athens, 10676 Athens, Greece

ARTICLE INFO

Article history:
Received 23 December 2015
Received in revised form
5 February 2016
Accepted 29 February 2016
Available online 19 April 2016

Keywords:
Ablation
Accessory pathway
Aortic cusps

ABSTRACT

Data regarding catheter ablation of anteroseptal accessory pathways through the aortic cusps are limited. We describe two cases of true para-Hisian accessory pathways successfully ablated from the aortic cusps (right coronary cusp and non-coronary cusp, respectively) along with a review of the current literature. Due to the close proximity to the atrioventricular node and the high risk of complication, mapping of the aortic cusps should always be considered in the case of anteroseptal accessory pathways. Anteroseptal accessory pathways can be safely and effectively ablated from the aortic cusps with good long-term outcomes.

Contents

1. Introduction

Catheter ablation of accessory pathways (APs) can be challenging depending on the location of the AP. Anteroseptal APs are rare but associated with lower success rates and higher incidence of atrioventricular (AV) block [1,2]. Data regarding the electrocardiographic and electrophysiological characteristics as well as the safety and efficacy of catheter ablation of anteroseptal APs through the aortic cusps are limited [3–18]. We describe two cases of para-Hisian APs successfully ablated from the aortic cusps along with a detailed review of the current literature.

2. Cases

2.1. Case 1

A 23-year-old woman with known pre-excitation syndrome and symptomatic supraventricular tachycardia was referred for radiofrequency (RF) catheter ablation. Electrocardiogram findings demonstrated overt pre-excitation with positive delta waves in leads I, II, III, aVF, V1, and V2 (Fig. 1A). An electrophysiological study was performed in a fasting state under conscious sedation.

* Corresponding author. Tel.: +30 2132041466; fax: +30 2132041344.
E-mail address: k.letsas@gmail.com (K.P. Letsas).

http://dx.doi.org/10.1016/j.joa.2016.02.010

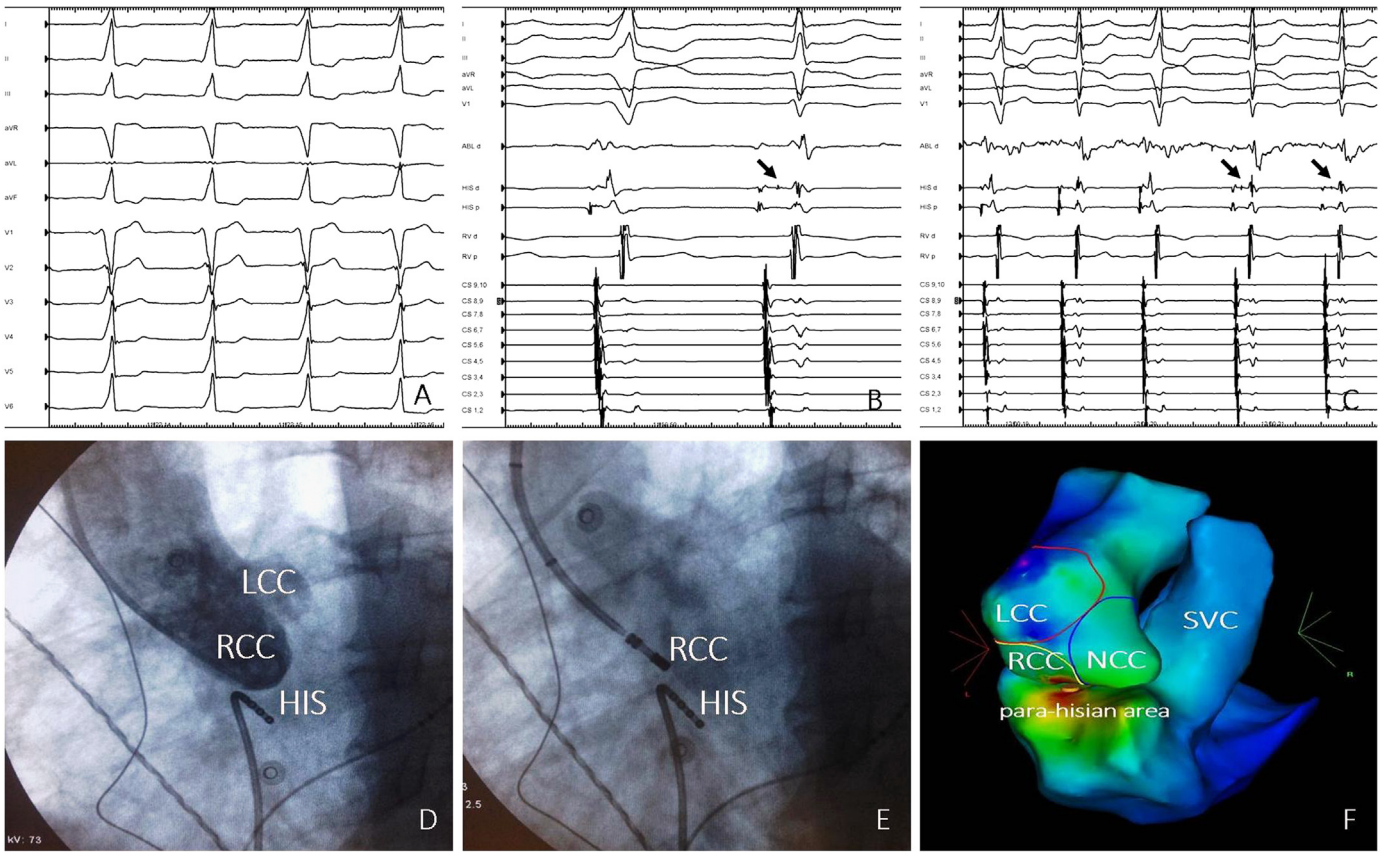

Fig. 1. (A) Twelve-lead ECG strip showing overt pre-excitation; (B) Mapping in sinus rhythm (antegrade conduction) showing the earliest ventricular activity at the RCC (ABL d) in relation to the right para-Hisian area (HIS d). Catheter manipulation within the RCC led to mechanical block of the AP and revealed the His-bundle deflection in the right side (arrow in the HIS d recordings); (C) RF energy delivery led to permanent loss of pre-excitation. At the successful ablation site, the ventricular electrogram is significantly larger than the atrial electrogram confirming the RCC position; (D) Aortography in LAO projection showing the anatomical relationships of the RCC, the LCC, and the para-Hisian area (HIS catheter); (E) Fluoroscopic image in LAO projection showing the position of the ablation catheter within the RCC; (F) Electroanatomic activation mapping during sinus rhythm showing the earliest ventricular activation sites in the RCC and the right para-Hisian area (red color). ECG: electrocardiogram; LAO: left anterior oblique; LCC: left coronary cusp; NCC: non-coronary cusp; RCC: right coronary cusp; RF: radiofrequency; SVC: superior vena cava.

All antiarrhythmic drugs were stopped for a minimum of five half-lives before the procedure. After obtaining femoral vascular access, a decapolar catheter was placed into the coronary sinus, and quadripolar recording catheters were placed at the His and right ventricular apex positions. The presence of a para-Hisian AP was easily demonstrated during antegrade mapping in sinus rhythm (delta wave-V = 0 ms). Because of the close proximity to the AV node and the high risk of complication, mapping of the aortic cusps through a retrograde aortic approach was subsequently performed under systemic anticoagulation with intravenous administration of heparin. Coronary angiography–aortography and three-dimensional (3-D) electroanatomical mapping (Carto 3, Biosense Webster) was performed to establish the location of the coronary arteries and to delineate the anatomical features of the aortic cusps. A 3.5-mm irrigated tip ablation catheter (ThermoCool SmartTouch, Biosense Webster) was used for mapping and RF current application. During mapping in sinus rhythm (antegrade conduction), the earliest ventricular activity recorded at the right coronary cusp (RCC) preceded the delta wave by 20 ms (Fig. 1B). At this site, catheter manipulation led to mechanical block of the AP (Fig. 1B). RF energy titration (from 25 to 35 W, 43 °C) led to permanent loss of pre-excitation without any complications (Fig. 1C). The morphology of the intracardiac electrograms in correlation with standard fluoroscopic (Fig. 1D and E) and electroanatomical (Fig. 1F) images confirmed the exact location of the mapping catheter within the RCC near the RCC-non-coronary cusp (NCC) junction. As shown in Fig. 1C, at the successful ablation site, the ventricular electrogram was significantly larger than the atrial electrogram confirming the RCC position [19,20]. The close anatomical proximity of the RCC and right para-Hisian area is demonstrated in 3-D electroanatomical activation mapping (earliest ventricular activity with respect to delta wave onset) (Fig. 1E). The distance between the RCC and the right para-Hisian area was less than 10 mm. The patient is free from arrhythmias 6 months after the procedure.

2.2. Case 2

A 31-year-old man with pre-excitation syndrome and atrial fibrillation was referred for RF catheter ablation. Electrocardiogram findings demonstrated overt pre-excitation with positive delta waves in leads I, II, aVF, V1, and V2. Lead III displayed a negative delta wave (Fig. 2A). An electrophysiological study was performed as previously described in case 1. Antegrade mapping revealed the presence of a para-Hisian AP (delta wave-V = −10 ms). Low-energy application (15 W) delivered with a 7F deflectable ablation catheter with a 4-mm tip electrode resulted in transient AV block. Electroanatomical mapping of the aortic cusps through a retrograde aortic approach was subsequently performed. During antegrade mapping, the earliest ventricular activity recorded at the NCC preceded the delta wave by 25 ms (Fig. 2B). A fragmented ventricular electrogram was noted at this site. RF application (30 W, 43 °C with a 3.5-mm irrigated tip ablation catheter [ThermoCool SmartTouch, Biosense Webster]) led to permanent loss of pre-excitation without any complications (Fig. 2C). The morphology of the intracardiac electrograms in

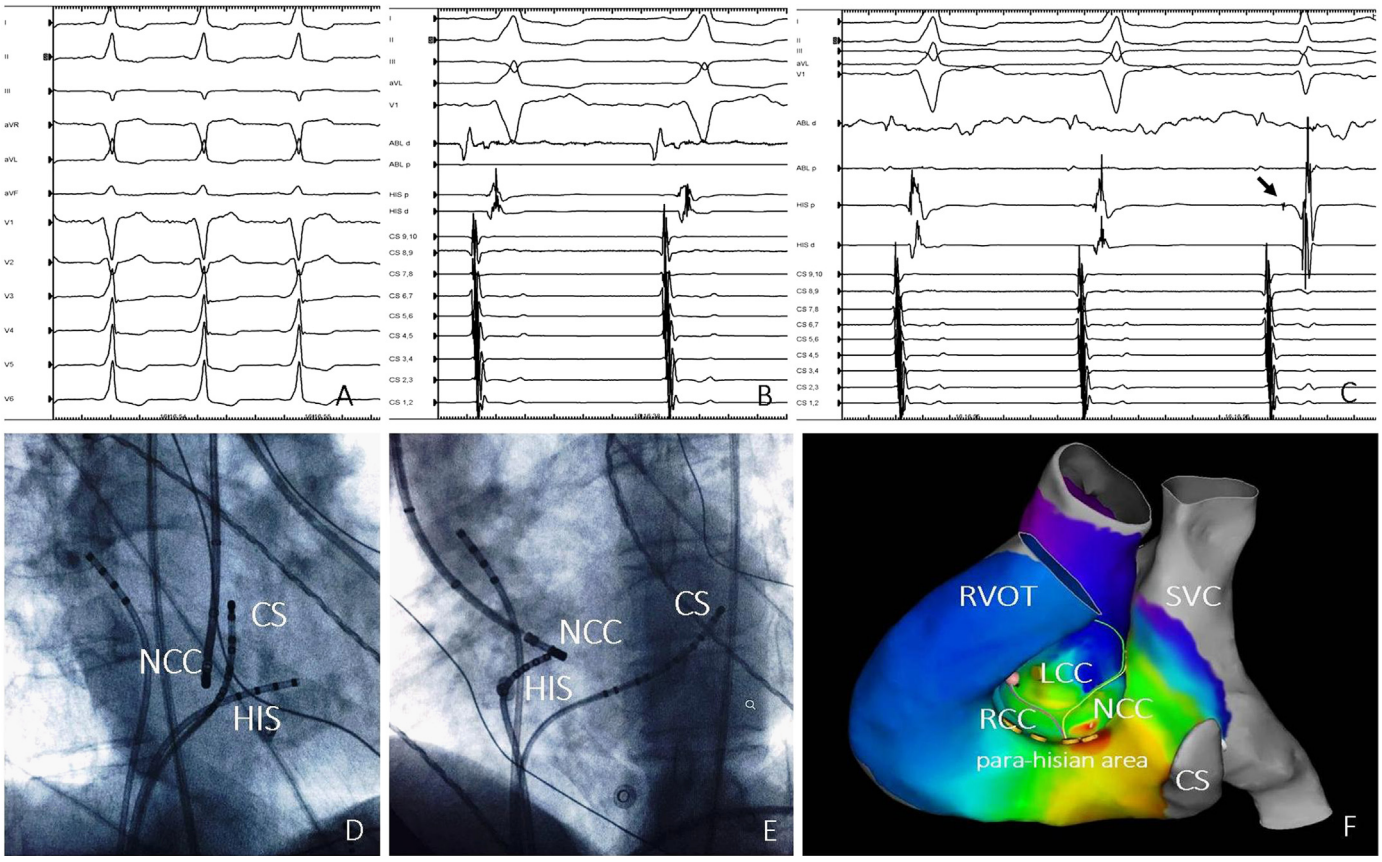

Fig. 2. (A) Twelve-lead ECG strip showing overt pre-excitation; (B) Mapping in sinus rhythm (antegrade conduction) showing the earliest ventricular activity at the NCC (ABL d) in relation to the right para-Hisian area (HIS p); (C) RF energy delivery led to permanent loss of pre-excitation and revealed a clear His-bundle deflection in the right side (arrow in the HIS p recordings); (D) Fluoroscopic image in RAO projection showing the position of the ablation catheter within the NCC in relation to the right para-Hisian area (HIS catheter); (E) Fluoroscopic image in the LAO projection showing the position of the ablation catheter within the NCC in relation to the right para-Hisian area (HIS catheter); (F) Electroanatomic activation mapping during sinus rhythm showing the earliest ventricular activation sites in NCC and the right para-Hisian area (red color). CS: coronary sinus; ECG: electrocardiogram; LAO: left anterior oblique; LCC: left coronary cusp; NCC: non-coronary cusp; RAO: right anterior oblique; RCC right coronary cusp; RF: radiofrequency; RVOT: right ventricular outflow tract; SVC: superior vena cava.

correlation with standard fluoroscopic (Fig. 2D and E) and electroanatomical (Fig. 2F) images confirmed the position of the mapping catheter at the NCC. In particular, at the successful ablation site, the atrial electrogram was significantly larger than the ventricular electrogram confirming the NCC position [19,20]. Electroanatomical activation mapping demonstrated the close proximity of the earliest ventricular activation sites in the NCC and right para-Hisian area, respectively (Fig. 2E). The patient is free from arrhythmias 4 months after the procedure.

3. Discussion

We presented the electocardiographic and electrophysiological characteristics of two patients with para-Hisian APs successfully ablated from the RCC near the RCC–NCC junction and the NCC, respectively. A comprehensive literature search of relevant studies published in MEDLINE up to November 2015 was additionally conducted. Sixteen case studies [3–18] comprising 36 patients with septal APs successfully ablated through the aortic cusps were included in this analysis. In most of these cases, a right-sided approach was initially undertaken and had been unsuccessful highlighting the importance of recognizing the presence of an aortic cusp pathway when present. As shown in Table 1, the majority of APs were located at the NCC (66.6%) and the RCC (19.4%), and less commonly at the left coronary cusp (LCC) (5.5%), at the RCC–NCC commissure (5.5%), and at the LCC–NCC commissure (2.7%). The delta waves were usually positive in lateral (I, aVL) and inferior leads (II, III, aVF), while varied in lead V1 (positive, isoelectric, negative). The polarity of the delta wave in lead V1 was not site specific. Although NCC APs ($n=4$) (*posterior location*) displayed more commonly positive delta waves in lead V1, there were also NCC APs ($n=2$) exhibiting negative delta waves. RCC APs (anterior location) displayed negative delta waves in lead V1. For APs located in the NCC, the delta wave in lead III was less positive than that in lead II. The transition zone was usually in lead V3 (less commonly in leads V2 and V4). Both para-Hisian AP cases described in our study displayed positive delta waves in leads I, aVL, II, aVF, and V1. In case 1, the delta wave in lead III was less positive than that in lead II, while in case 2 the delta wave in lead III was negative. As shown in Table 1, RF energy delivered with irrigated and non-irrigated tip catheters was most commonly used. Cryoablation was used in few cases (2 out 36). The incidence of AV block was very low (1 out of 36 cases, 2.7%). No other complications were reported.

The data regarding the efficacy and safety of the conventional right-sided catheter ablation approach of anteroseptal APs are controversial. There are studies demonstrating excellent long-term outcomes without any damage of the AV node [21,22], while other studies report lower success rates and higher incidence of AV block [1,2,23]. In the largest case series up to now, Xu et al. compared the safety, efficacy, and long-term outcome of the two different ablation approaches for para-Hisian APs [3]. RF energy delivered at the NCC had a higher success rate (11/12 vs. 5/12) and a lower complication rate (0/12 vs. 4/12) compared with the right anteroseptal approach.

Table 1
Clinical, electrocardiographic, and electrophysiological characteristics of septal APs successfully ablated from the aortic cusps.

Author/Date	Patients	Age (years)	ECG	AP location	Successful ablation site	Energy used, Energy settings, Type of ablation catheter	Complications
Xu et al. (2015)	12	14-69	NR	Para-Hisian AP	NCC	– RF energy – 15–40 W – Non-irrigated tip	None
Liao et al. (2015)	1	15	– Positive delta wave in leads I, aVL, II, III, aVF (II > III) – Negative delta wave in lead V1 – Transition zone in lead V3	Para-Hisian AP	RCC	– RF energy – 30 W – NR	None
Tanıdır et al. (2015)	1	17	– Positive delta wave in leads I, II, III, aVF – Negative delta wave in leads V1–V2	Right anteroseptal AP	NCC	– RF energy – NR – NR	None
Laranjo et al. (2015)	1	NA	NA	Left anterior AP	LCC–NCC junction	– RF energy – NA – NA	None
DeMazumder et al. (2014)	1	31	– Positive delta waves in leads I, aVL, aVF – Positive delta wave in lead V1 – Transition zone in lead V3	Right anteroseptal AP	RCC–NCC junction	– RF energy – 30 W – Irrigated tip	None
Oloriz et al. (2014)	1	13	– Positive delta waves in leads I, aVL, II, III, aVF – Negative delta wave in lead V1 – Transition zone in lead V3	Right anteroseptal AP	RCC	– RF energy – 15–20 W –Irrigated tip	None
Ozcan et al. (2013)	1	38	– Positive delta waves in leads I, II, III, aVF – Positive delta wave in lead V1 – Transition zone in lead V3	Right anteroseptal AP	NCC	– RF energy – NR – Irrigated tip	None
Baszko et al. (2012)	1	27	– Positive delta waves in leads I, II, III, aVF (II > III) – Negative delta wave in lead V1 – Transition zone in lead V3	Right anteroseptal AP	NCC	– RF energy – 45 W, 48 °C – Non-irrigated tip	None
Park et al. (2013)	7	NR	NR	Right midseptal and anteroseptal APs	NCC=2 RCC=5	– RF energy – 50 W, 60 °C – Non-irrigated tip	- AV block 48 h after RCC AP- Arrhythmia recurrence or WPW on ECG in 2 patients

Kobayashi et al. (2012)	1	15	– Positive delta waves in leads I, aVL, II, III, aVF – rS configuration in lead III – Positive delta wave in lead V1 – Transition zone in lead V4	Right anteroseptal AP	NCC	– RF energy – 20 W, 50 °C – Irrigated tip	None
Wilsmore et al. (2012)	1	42	Concealed	Para-Hisian AP	LCC	– RF energy- Irrigated tip – 15–35 W – Irrigated tip	None
Godin et al. (2011)	1	26	– Positive delta waves in leads I, II, III, aVF (II > III) – Isoelectric delta wave in lead V1 – Transition zone in lead V2	Para-Hisian AP	LCC	– RF energy	None
Suleiman et al. (2011)	3	Patient 1: 17 Patient 2: 31 Patient 3: 18	Patient 1: – Less positive delta waves in lead III than in lead II Patient 2: – NR Patient 3: – The delta wave was less positive in lead III in comparison to lead II	Right anteroseptal AP	NCC	Patient 1: - RF energy – 20–50 W 60 °C – Non-irrigated tip Patient 2: – Cryoablation (−70 °C). – RF energy was delivered at the successful siteas “insurance” burns Patient 3: – Cryoablation (−70 °C)	None
Balasundaram et al. (2009)	1	< 1 year (4th month)	Concealed AP	Para-Hisian AP	NCC	– RF energy – 25 W, 55 °C – Non-irrigated tip	None
Huang et al. (2006)	1	29	– Positive delta waves in leads I, II, III and aVF – Positive delta waves in leads V1 and V2 – Transition zone in lead V4	Right anteroseptal AP	NCC	– RF energy – 20-35 W, 55 °C – Non-irrigated tip	None
Tada et al. (2003)	1	51	Concealed AP	Para-Hisian AP	NCC	– RF energy – 35 W, 55 °C – Non-irrigated tip	None

AP: accessory pathway; AV: atrioventricular; ECG: electrocardiogram; LCC: left coronary cusp; NA: not available; NCC: non-coronary cusp; NR: not reported; RCC right coronary cusp; RF: radiofrequency; WPW: Wolff-Parkinson-White

From an electrophysiological point of view, it is essential to understand the importance of the central position of the aortic valve and its relationship with adjacent structures. The aortic valve is directly related with both atria, the interatrial septum, the right ventricular outflow tract, the aortomitral continuity, the pulmonary valve, and the conduction system [20,24]. The RCC lies immediately posterior to the relatively thick posterior wall of the right ventricular outflow tract. The LCC is also related to the posterior wall of the right ventricular outflow tract, but more posteriorly continuous with the anterior leaflet of the mitral valve as the aortomitral continuity. The NCC is located more posterior in relation to other cusps and forms the superior margin of the interatrial septum. As the conduction system penetrates to the left, it becomes located at the base of the interleaflet triangle between the NCC and the RCC [24]. The latter possibly explains that the majority of septal APs were successfully ablated at the NCC, RCC, or RCC–NCC junction (33 out of 36 APs). These APs are possibly electrically active connections between the ventricular myocardium (just below and extending above the aortic cusps) and atrial myocardium (adjacent interatrial septum). The mechanical block of the AP seen in case 1 supports this notion. Myocardial sleeves have been demonstrated to extend beyond the plane of attachment of the semilunar valves into the aorta. In autopsied hearts, myocardial extensions were noted above the RCC in 55%, LCC in 24%, non-coronary/posterior cusp in 0.66%, intercuspally in 49% (2.2 ± 1.1 mm), and in the cusps in 2.2% of cases [25]. Yamada et al. suggested that the NCC exhibits direct musculature connection with the His-bundle region and the mid-interatrial septum in the left atrium [26]. In animal studies, RF catheter ablation within the NCC has been shown to create lesions at the left atrial septum located between the floor of the fossa ovalis and the mitral annulus. These findings are strongly indicating the close anatomical proximity of the NCC with the interatrial septum [27].

The exact location of the APs within the cusps is difficult to determine. The majority of studies used coronary angiography, and less commonly electroanatomical mapping. The morphology of local atrial and ventricular electrograms may be additionally used [1,2]. Mapping within the RCC typically shows a large ventricular electrogram, while the atrial electrogram is small and often absent. The largest atrial electrograms are recorded in the NCC. A ventricular signal may or may not be present. Electrograms obtained from the LCC are the most variable of the aortic cusps [19,20]. Intracardiac echocardiography may add important information on this topic. Integration of cardiac computed tomography or magnetic resonance imaging with 3-D electroanatomical mapping may also provide useful anatomical information during catheter ablation.

In previous studies, there were no embolic events following RF ablation within the cusps [3–18]. However, based on the clinical experience during ablation of other left sided arrhythmias, a more prudent strategy is to use cooled RF ablation or cryoablation within the aortic cusps in order to minimize the risk of thrombus formation [27].

4. Conclusion

In conclusion, anteroseptal APs including true para-Hisian APs can be safely and effectively ablated from the aortic cusps. Compared with the ablation at the right anteroseptal area, RF delivered at the aortic cusps has a higher immediate success, lower complication rate, and good long-term outcome. The aortic cusps should always be considered as the initial target for ablation of para-Hisian APs. Electroanatomic mapping may add important information confirming the anatomical relationship of the right anteroseptal area and the aortic cusps.

Conflict of interest

All authors declare no conflict of interest related to this study.

References

[1] Calkins H, Yong P, Miller JM, et al. Catheter ablation of accessory pathways, atrioventricular nodal reentrant tachycardia, and the atrioventricular junction: final results of a prospective, multicenter clinical trial. The Atakr Multicenter Investigators Group. Circulation 1999;99:262–70.
[2] Tai CT, Chen SA, Chiang CE, et al. Electrocardiographic and electrophysiologic characteristics of anteroseptal, midseptal, and para-Hisian accessory pathways. Implication for radiofrequency catheter ablation. Chest 1996;109:730–40.
[3] Xu G, Liu T, Liu E, et al. Radiofrequency catheter ablation at the non-coronary cusp for the treatment of para-hisian accessory pathways. Europace 2015;17:962–8.
[4] Tanıdır İC, Özyılmaz İ, Ünsal S, et al. Catheter ablation of the anteroseptal accessory pathway from the non-coronary aortic cusp in a pediatric patient. Anatol J Cardiol 2015;15:259–60.
[5] Liao Z, Zhan X, Wu S. Successful radiofrequency ablation of a parahisian accessory pathway from the right coronary cusp. Int J Cardiol 2015;186:41–2.
[6] Laranjo S, Oliveira M, Trigo C. Successful catheter ablation of a left anterior accessory pathway from the non-coronary cusp of the aortic valve. Cardiol Young 2015;25:1200–2.
[7] DeMazumder D, Barcelon B, Cockrell J, et al. Ablation of an anteroseptal accessory pathway from the aortic root using electroanatomic mapping. Heart Rhythm 2014;11:2122–3.
[8] Oloriz T, Gulletta S, Della Bella P. Successful radiofrequency ablation of an anteroseptal accessory pathway from the right coronary cusp. Europace 2014;16:1204.
[9] Ozcan C, Barrett CD. Utility of intracardiac echocardiography for catheter ablation of an anteroseptal accessory pathway from the non-coronary aortic cusp. Int J Cardiol 2013;167:e153–5.
[10] Park J, Wi J, Joung B, et al. Prevalence, risk, and benefits of radiofrequency catheter ablation at the aortic cusp for the treatment of mid- to anteroseptal supra-ventricular tachyarrhythmias. Int J Cardiol 2013;167:981–6.
[11] Hocini M, Shah AJ, Denis A, et al. Noninvasive 3D mapping system guided ablation of anteroseptal pathway below the aortic cusp. Heart Rhythm 2013;10:139–41.
[12] Kobayashi D, Arya SO, Singh HR. Successful ablation of antero-septal accessory pathway in the non-coronary cusp in a child. Indian Pacing Electrophysiol J 2012;12:124–30.
[13] Wilsmore BR, Tchou PJ, Kanj M, et al. Catheter ablation of an unusual decremental accessory pathway in the left coronary cusp of the aortic valve mimicking outflow tract ventricular tachycardia. Circ Arrhythm Electrophysiol 2012;5:e104–8.
[14] Suleiman M, Brady PA, Asirvatham SJ, et al. The noncoronary cusp as a site for successful ablation of accessory pathways: electrogram characteristics in three cases. J Cardiovasc Electrophysiol 2011;22:203–9.
[15] Godin B, Guiot A, Savoure A, et al. The left coronary cusp as an unusual location for accessory pathway ablation. Heart Rhythm 2011;8:1769–72.
[16] Balasundaram R, Rao H, Asirvatham SJ, et al. Successful targeted ablation of the pathway potential in the noncoronary cusp of the aortic valve in an infant with incessant orthodromic atrioventricular reentrant tachycardia. J Cardiovasc Electrophysiol 2009;20:216–20.
[17] Huang H, Wang X, Ouyang F, et al. Catheter ablation of anteroseptal accessory pathway in the non-coronary aortic sinus. Europace 2006;8:1041–4.
[18] Tada H, Naito S, Nogami A, et al. Successful catheter ablation of an anteroseptal accessory pathway from the noncoronary sinus of Valsalva. J Cardiovasc Electrophysiol 2003;14:544–6.
[19] Sasaki T, Hachiya H, Hirao K, et al. Utility of distinctive local electrogram pattern and aortographic anatomical position in catheter manipulation at coronary cusps. J Cardiovasc Electrophysiol 2011;22:521–9.
[20] Tabatabaei N, Asirvatham SJ. Supravalvular arrhythmia: identifying and ablating the substrate. Circ Arrhythm Electrophysiol 2009;2:316–26.
[21] Haissaguerre M, Marcus F, Poquet F, et al. Electrocardiographic characteristics and catheter ablation of parahissian accessory pathways. Circulation 1994;90:1124–8.
[22] Schluter M, Kuck KH. Catheter ablation from right atrium of anteroseptal accessory pathways using radiofrequency current. J Am Coll Cardiol 1992;19:663–70.
[23] Yeh SJ, Wang CC, Wen MS, et al. Characteristics and radiofrequency ablation therapy of intermediate septal accessory pathways. Am J Cardiol 1994;73:50–6.
[24] Suleiman M, Asirvatham SJ. Ablation above the semilunar valves: when, why, and how? Part II Heart Rhythm 2008;5:1625–30.
[25] Gami AS, Noheria A, Lachman N, et al. Anatomical correlates relevant to ablation above the semilunar valves for the cardiac electrophysiologist: a study of 603 hearts. J Interv Card Electrophysiol 2011;30:5–15.
[26] Yamada T, Huizar JF, McElderry HT, et al. Atrial tachycardia originating from the noncoronary aortic cusp and musculature connection with the atria: relevance for catheter ablation. Heart Rhythm 2006;3:1494–6.
[27] d'Avila A, Thiagalingam A, Holmvang G, et al. What is the most appropriate energy source for aortic cusp ablation? A comparison of standard RF, cooled-tip RF and cryothermal ablation J Interv Card Electrophysiol 2006;16:31–8.